Fuzzy PID Controller Analysis for the Hexacopter Aircraft Using Simulink Simulation

Jiahui Feng[1], Yuhui Luo[2], Zixian Huang[3], Rueiyuan Wang[4], Rongguei Tsai[5], Raojun Luo[6], Chaoxiong Su[7], Hosheng Chen[*8]

[1,2,3,5,6,7,8]School of Sciences, Guangdong University of Petrochem Technology (GDUPT), Maoming 525000, China

[5]Guangdong University of Science and Technology, China

*Corresponding author

Abstract— This study aims to investigate the control benefits of rotary wing aircraft systems through the Simulink simulation platform. A hexacopter aircraft is a small unmanned aerial vehicle (UAV) powered by the operation of six rotors, which has important theoretical and practical application value. Firstly, the body structure and working principle of the hexacopter aircraft are proposed. Then, a mathematical model of the hexacopter aircraft is established to support the design of subsequent control strategies. Next, compare the differences between the classical PID controller design and the fuzzy PID controller design methods for aircraft control systems and verify them through simulation experiments. The simulation results show that compared with the classical PID controller, the fuzzy PID controller can stabilize the aircraft at the target position faster when subjected to various types of disturbances and have good practicality, stability, speed, and accuracy. Based on this, future research can further explore the application of other advanced control strategies in aircraft control systems and their prospects in practical engineering.

I. INTRODUCTION

Nowadays, various aircraft are gradually popularized in various application fields of human beings, such as post-disaster rescue [8, 10], water quality sampling [5], military logistics [11], aerial photography [9], and other fields, playing an important role. With the continuous development of aircraft, the attention to their related products in today's society is gradually increasing. Therefore, more and more different types of aircraft are appearing on the market. The research object of this article, the hexacopter aircraft, is one of its derivative products.

The hexacopter arm of this study is installed according to the layout of a conventional X-shaped body, with the motor components and propeller distributed in the same position. The propeller has a fixed pitch, and although the angle between the rotating plane and the fuselage cannot be changed arbitrarily, the reverse torque can be balanced by changing the direction of adjacent motors. The six motors of the hexacopter control the attitude and altitude changes by changing the speed. Number the motors as M1~M6, and the direction of rotation of the motors is shown in Figure 1. [1,3,4,14,15]
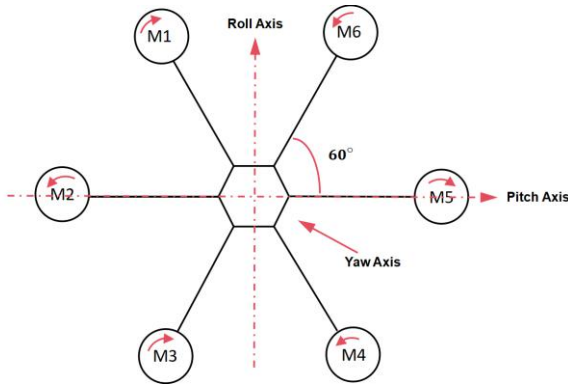
Fig.1 Schematic diagram of the rotational posture of the hexacopter motor

When the six motors of a quadcopter operate in synergy, the aircraft can achieve various motion controls such as roll, pitch, translation, yaw, and hover during flight [7]. The flight control of drones is usually achieved through a built-in flight control system, which calculates and adjusts the rotor speed based on data provided by sensors such as gyroscopes, accelerometers, and compasses to achieve stable flight.

The purpose of this article is to study the motion control system of a hexacopter aircraft, establish mathematical models for the kinematics and dynamics of the hexacopter, and consider the attitude and altitude information of the hexacopter. The main approach is based on the functions of MATLAB software, classical PID control, and fuzzy PID control [2, 6, 12], as well as the anti-interference attitude controller designed with anti-interference control ideas [13]. The mathematical models derived from mathematical and physical theories are imported into Matlab software for simulation, which can effectively test the stability, speed, and accuracy of the six-rotor aircraft system, obtain relevant data, and compare the data of classical PID control and fuzzy PID control to verify the superiority of the fuzzy PID control system in all aspects.

II. ESTABLISH MATHEMATICAL MODEL FOR HEXACOPTER AIRCRAFT

2.1 Coordinate System and Attitude Representation of Hexacopter Drones

The coordinate system of a hexacopter aircraft is divided into a ground coordinate system and an aircraft coordinate system, mainly using a three-dimensional Cartesian coordinate system to define the two coordinate systems of the drone. The ground coordinate system refers to the coordinates of the motion state and spatial position relative to the ground. The X-Y-Z inertial coordinates of the aircraft are taken in the north-east ground direction of the earth and represented by G. The aircraft coordinate system is represented by B, with the center of the aircraft represented by OB. The X-Y-Z of the aircraft coordinate system corresponds to the front right bottom direction of the hexacopter aircraft. The transformation between the ground coordinate system and the aircraft coordinate system is shown in Figure 2.
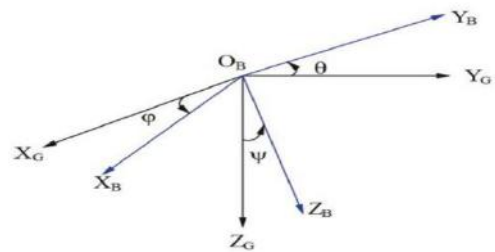
Fig.2: Transformation of Ground Coordinates Systems and Aircraft Coordinate Systems

The rotation angle of the aircraft coordinate system around the X-Y-Z axis of the ground coordinate system can obtain three Euler angles, namely yaw angle φ, roll angle θ, and pitch angle ψ. The Euler angle is commonly used to represent the relationship between the ground coordinate system and the aircraft coordinate system and is an intuitive attitude representation method for UAV. According to Euler's theorem, the rotation of a rigid body around a fixed point is the synthesis of several finite rotations around that point. Therefore, the motion of a rigid body rotating around a fixed point can be decomposed into a series of individual rotations around that point, with the rotation angle being Euler's angle. Thus, the attitude matrix is represented by the product of three basic rotation matrices, making the ground coordinate system and the aircraft coordinate system exactly the same.

When XB rotates around the XG axis, the obtained yaw angle is φ, and the transformation matrix RX (φ) is:

$$R_X(\varphi)=\begin{bmatrix} 1 & 0 & 0 \\ 0 & \cos\varphi & -\sin\varphi \\ 0 & \sin\varphi & \cos\varphi \end{bmatrix}$$

When YB rotates around the YG axis, the roll angle θ is obtained, and the transformation matrix Ry (θ) is obtained as follows:

$$R_X(\theta)=\begin{bmatrix} \sin\theta & 0 & -\sin\theta \\ 0 & 1 & 0 \\ \sin\theta & 0 & \cos\theta \end{bmatrix}$$

When ZB rotates around the ZG axis, the resulting pitch angle is denoted as ψ. The transformation matrix RZ (ψ) is obtained as follows:

$$R_X(\psi)=\begin{bmatrix} \cos\psi & \sin\psi & 0 \\ -\sin\psi & \cos\psi & 0 \\ 0 & 0 & 1 \end{bmatrix}$$

When the hexacopter rotates in the three-axis position during flight, according to Newton's second theorem M=J$\dot\omega$, the conversion relationship of angular velocity S＝$\begin{bmatrix} \dot\varphi & \dot\theta & \dot\psi \end{bmatrix}$ in the ground coordinate system can be obtained as follows:

$$R(\psi、\theta、\varphi) = \begin{bmatrix} \cos\psi\cos\theta & \cos\psi\sin\theta\sin\varphi - \sin\psi\cos\varphi & \cos\psi\sin\theta\cos\varphi + \sin\psi\sin\varphi \\ \sin\psi\cos\theta & \cos\psi\cos\varphi + \sin\psi\sin\theta\sin\varphi & \sin\psi\sin\theta\cos\varphi - \cos\psi\sin\varphi \\ -\sin\theta & \cos\theta\sin\psi & \cos\theta\cos\varphi \end{bmatrix} \quad (1)$$

2.2 Mathematical Model of Hexacopter Aircraft

The hexacopter aircraft in this article is a mathematical model of the "X" type, but in actual flight, it is subject to uncertain factors such as its own gravity, air resistance, and changes in its own torque. If the flight speed of the aircraft is relatively low, the following assumptions are made to simplify the modeling of the aircraft:

(1) Hexacopter aircraft should be treated as rigid bodies, and the structural elasticity and deformation of the body should be ignored.

(2) The mass and moment of inertia of the aircraft are assumed to be almost constant, only subjected to gravity and propeller tension, ignoring unknown disturbances.

(3) The geometric center of the hexacopter is not only the same as but also coincides with the position of gravity.

(4) Neglecting the influence of the Earth's rotation and revolution on the forces acting on a hexacopter UAV.

According to physical theory, force analysis shows that the lift is mainly affected by the body's gravity and the generated lift. Lift is generated by six motors driving the rotor to rotate, namely F1, F2, F3, F4, F5, and F6. The combined force of a six rotor UAV is F; the angular velocity is ω, the moment of inertia is J, the body weight is m, the velocity is v, and the resultant moment is M. The lift generated by the hexacopter is defined as UZ, the lift coefficient is defined as b, and the arm length is defined as L. Define E=[xyz] T as the position motion vector of the hexacopter body in the ground coordinate system, and $\ddot{E}$ as the acceleration vector; $\omega = \begin{bmatrix} p & q & r \end{bmatrix}^T$ is the vector on the X-Y-Z axis in the ground coordinate system,

and $\dot{\omega}$ is the angular acceleration. When the hexacopter undergoes translational motion during three-axis flight, according to Newton's second law F=ma, it can be obtained that:

$$\begin{bmatrix} \ddot{x} \\ \ddot{y} \\ \ddot{z} \end{bmatrix} = F + \begin{bmatrix} 0 \\ 0 \\ mg \end{bmatrix} \quad (2)$$

When the lift direction generated by the six rotors of a hexacopter is consistent and perpendicular to the ground coordinate ZG direction, then:

$$U_z＝F＝F1 + F2 + F3 + F4 + F5 + F6$$
$$＝b(\omega_1^2 + \omega_2^2 + \omega_3^2 + \omega_4^2 + \omega_5^2 + \omega_6^2) \quad (3)$$

According to F=[0 0 -UZ]T as the vector of the total lift of the hexacopter, the mathematical model of the nonlinear kinematics of the hexacopter aircraft is obtained by substituting equations (1) and (2) as follows:

$$\begin{cases} \ddot{x} = -\dfrac{(\cos\psi\sin\theta\cos\varphi+\sin\psi\sin\varphi)U_z}{m} \\ \ddot{y} = -\dfrac{(\cos\psi\sin\theta\cos\varphi-\sin\psi\sin\varphi)U_z}{m} \\ \ddot{z} = -\dfrac{(\cos\theta\cos\varphi)U_z-mg}{m} \end{cases} \quad (4)$$

When the hexacopter rotates in the three-axis position during flight, according to Newton's second theorem M=J$\dot\omega$, the conversion relationship of the angular velocity S＝$[\dot\varphi \quad \dot\theta \quad \dot\psi]^T$ in the ground coordinate system can be obtained as follows:

$$\begin{bmatrix} \dot\varphi \\ \dot\theta \\ \dot\psi \end{bmatrix} = \begin{bmatrix} 1 & \sin\varphi\tan\theta & \cos\varphi\tan\theta \\ 0 & \cos\varphi & -\sin\varphi \\ 0 & \sin\varphi\sec\theta & \cos\varphi\sec\theta \end{bmatrix}\begin{bmatrix} p \\ q \\ r \end{bmatrix} =$$

$$\begin{bmatrix} \dfrac{p\sin\theta+q\sin\varphi\sin\theta+r\cos\varphi\sin\theta}{\cos\theta} \\ q\cos\theta - r\sin\varphi \\ \dfrac{q\sin\varphi+r\cos\theta}{\cos\theta} \end{bmatrix} \quad (5)$$

When a hexacopter aircraft performs roll, pitch, and yaw movements during flight, according to the conservation of angular momentum M=Ia, the relationship between the rotational moments M_X, M_Y, M_Z in the x, y, z directions of the body coordinate axes and the rotational inertia I_X, I_Y, I_Z can be analyzed. It can be concluded that:

$$\begin{cases} M_X = I_X\dot{p} + qr\,(I_Y - I_Z) = I_X\ddot{\varphi} + \dot{\theta}\dot{\psi}(I_Y - I_Z) \\ M_Y = I_Y\dot{q} + pr\,(I_Z - I_X) = I_Y\ddot{\theta} + \dot{\psi}\dot{\varphi}(I_Z - I_X) \quad (6) \\ M_Z = I_Z\dot{p} + qp\,(I_X - I_Y) = I_Z\ddot{\psi} + \dot{\theta}\dot{\varphi}(I_X - I_Y) \end{cases}$$

The assumption of a hexacopter aircraft is decomposed from a mathematical model using four independent control channels. The variables for vertical (altitude) control input are defined as U_Z, lateral control input as U_H, pitch control input as U_F, and yaw input as U_P. From this, it can be inferred that the changes between each control channel and lift are:

$$\begin{cases} U_Z = F_1 + F_2 + F_3 + F_4 + F_5 + F_6 \\ U_H = F_1 + F_3 - F_4 - F_6 \\ U_F = F_6 - F_1 + F_3 - F_4 \quad (7) \\ U_P = F_1 + F_2 - F_3 - F_4 - F_5 + F_6 \end{cases}$$

Assuming all assumptions are met and wind resistance is ignored, based on the above calculations, the mathematical model of the theoretical dynamics of a hexacopter aircraft can be obtained as follows:

$$\begin{cases} \ddot{x} = -\dfrac{(\cos\psi\sin\theta\cos\varphi - \sin\psi\sin\varphi)U_Z}{m} \\ \ddot{y} = -\dfrac{(\sin\psi\sin\theta\cos\varphi - \cos\psi\sin\varphi)U_Z}{m} \\ \ddot{z} = -\dfrac{(\cos\theta\cos\varphi)U_Z - mg}{m} \\ \ddot{\varphi} = \dfrac{lU_H - \dot{\theta}\dot{\psi}(I_Y - I_Z)}{I_X} \quad (8) \\ \ddot{\theta} = \dfrac{lU_F - \dot{\varphi}\dot{\psi}(I_Z - I_X)}{I_Y} \\ \ddot{\psi} = \dfrac{lU_P - \dot{\theta}\dot{\varphi}(I_X - I_Y)}{I_Z} \end{cases}$$

The measured parameters of the hexacopter aircraft studied in this article are shown in Table 1.

Table 1 Parameters of Physical Measurement Values for Hexacopter Aircraft

Physical meaning	Parameter symbols	Parameter values
Total mass of hexacopter（kg）	m	6
Gravitational acceleration（m/s²）	g	9.8
Inertia of rotation around the X-axis（kg·m²）	I_X	0.6217
Inertia of rotation around the Y-axis（kg·m²）	I_Y	0.6217
Inertia of rotation around the Z-axis（kg·m²）	I_Z	1.0845
Hexacopter fuselage radius（1/2 wheelbase，m）	L	0.4025

III. CONTROL SYSTEM DESIGN AND FUZZY LOGIC ESTABLISHMENT

3.1 Control System Design

The control system is generally composed of multiple components, and the flow structure of the control system for a hexacopter aircraft is shown in Figure 3.
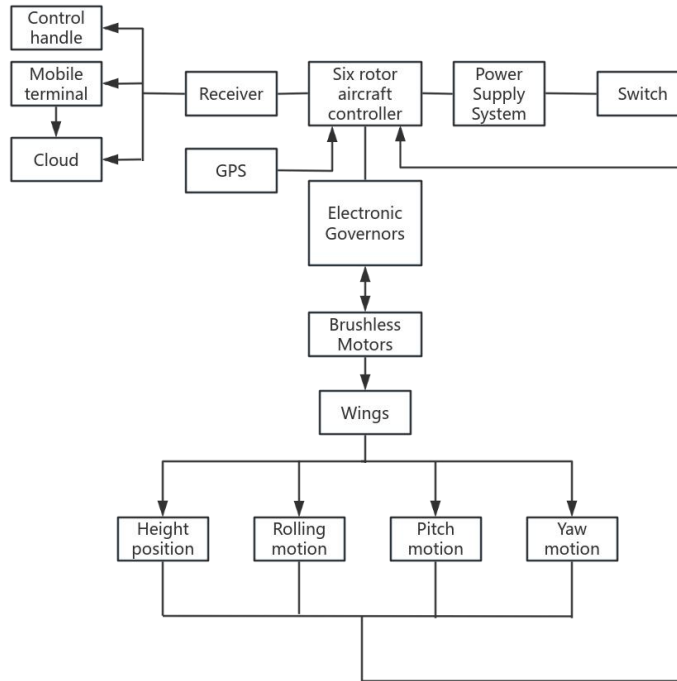
Fig.3 Flow Chart of Control System for Hexacopter Aircraft

3.2 Classic PID Control Principle

The most common control method in general control systems is classical PID control. The classic PID control system is shown in Figure 4.
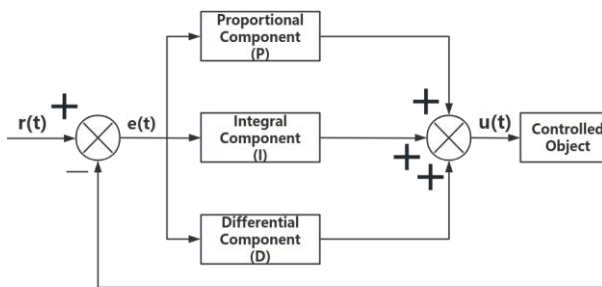
Fig.4 PID Control System Structure Diagram

The expression for the classic PID controller is:

$$e(t) = x(t) - y(t) \qquad (9)$$

$$u(t) = K_P e(t) + K_i \int_0^t e(t)dt + K_d \frac{d}{dt}e(t) \qquad (10)$$

In Figure 4, P, I, D represent proportional control, integral control, and differential control, respectively, corresponding to the proportional coefficient K_P, integral coefficient K_i, and differential coefficient K_d in equation (10). The proportional coefficient is the amplification factor of the difference between the preset value and the feedback value; the larger the proportional coefficient, the higher the adjustment sensitivity. The integral coefficient accumulates the difference between the preset value and the feedback value over time, but there is a significant lag. The differential coefficient is the rate of change of the research object, which can make corresponding adjustments in advance based on the rate of change of the difference.

3.3 PID Controller Transfer Function

After simplifying the model of the hexacopter aircraft, equation (8) can be obtained. The nonlinear equation can be processed to obtain a linearized equation. According to the system construction of this study, the six degrees of freedom of the aircraft can be reduced to four degrees of freedom, so only the height, pitch, roll, and yaw conditions of the vertical aircraft need to be considered during operation. The control variables for these four situations are represented by U_Z as variables perpendicular to X, Y, and Z, U_H as variables for roll, U_F as variables for pitch, and U_P as variables for yaw. The attitude change of the drone during flight is achieved through the variation of control angles ψ, θ, and φ. When $\cos\theta$ and $\cos\varphi$ are approximately 1 during flight, the drone is in hover or low-speed motion. The controller of a hexacopter aircraft

can convert the dynamic model into a state space expression through the LPV method, which is manifested as:

$$\begin{cases} \dot{X} = AX + BU_T \\ Y = CX + DU_T \end{cases} \quad (11)$$

where：

$$U_T = [U_Z \quad U_H \quad U_F \quad U_P]^T$$

$$X = [\dot{X} \quad \dot{Y} \quad \dot{Z} \quad \dot{\varphi} \quad \dot{\theta} \quad \dot{\psi} \quad \varphi \quad \theta \quad \psi]^T$$

$$Y = [\dot{Z} \quad \varphi \quad \theta \quad \psi]^T$$

$$A = \begin{bmatrix} 0 & 0 & 0 & 0 & 0 & 0 & 0 & 0 & 0 \\ 0 & 0 & 0 & 0 & 0 & 0 & 0 & 0 & 0 \\ 0 & 0 & 0 & 0 & 0 & 0 & 0 & 0 & 0 \\ 0 & 0 & 0 & 0 & 0 & 0 & 0 & 0 & 0 \\ 0 & 0 & 0 & 0 & 0 & 0 & 0 & 0 & 0 \\ 0 & 0 & 0 & 0 & 0 & 0 & 0 & 0 & 0 \\ 0 & 0 & 0 & 1 & 0 & 0 & 0 & 0 & 0 \\ 0 & 0 & 0 & 0 & 1 & 0 & 0 & 0 & 0 \\ 0 & 0 & 0 & 0 & 0 & 1 & 0 & 0 & 0 \end{bmatrix}$$

$$B = \begin{bmatrix} \frac{(\cos\psi\sin\theta\cos\varphi+\sin\psi\sin\varphi)}{m} & 0 & 0 & 0 \\ \frac{(\sin\psi\sin\theta\cos\varphi+\cos\psi\sin\varphi)}{m} & 0 & 0 & 0 \\ \frac{(\cos\theta\sin\varphi)}{m} & 0 & 0 & 0 \\ 0 & \frac{L}{I_X} & 0 & 0 \\ 0 & 0 & \frac{L}{I_Y} & 0 \\ 0 & 0 & 0 & \frac{L}{I_Z} \\ 0 & 0 & 0 & 0 \\ 0 & 0 & 0 & 0 \\ 0 & 0 & 0 & 0 \end{bmatrix}$$

$$C = \begin{bmatrix} 0 & 0 & 1 & 0 & 0 & 0 & 0 & 0 & 0 \\ 0 & 0 & 0 & 1 & 0 & 0 & 0 & 0 & 0 \\ 0 & 0 & 0 & 0 & 1 & 0 & 0 & 0 & 0 \\ 0 & 0 & 0 & 0 & 0 & 1 & 0 & 0 & 0 \end{bmatrix}$$

$$D = \begin{bmatrix} 0 & 0 & 0 & 0 \\ 0 & 0 & 0 & 0 \\ 0 & 0 & 0 & 0 \\ 0 & 0 & 0 & 0 \end{bmatrix}$$

The transfer function is obtained by applying Laplace transform to equation (11), which is:

$$G_1(s) = C[sl-A]^{-1} + D = \begin{bmatrix} \frac{\frac{(1)}{m}}{s} & 0 & 0 & 0 \\ 0 & \frac{\frac{L}{I_X}}{s} & 0 & 0 \\ 0 & 0 & \frac{\frac{L}{I_Y}}{s} & 0 \\ 0 & 0 & 0 & \frac{\frac{L}{I_Z}}{s} \end{bmatrix}$$

(12)

The brushless motor used in hexacopter drones is a small motor, and the inductance coefficient inside the brushless motor is relatively small. Thus, the inductance coefficient can be ignored. Therefore, using an approximate first-order inertia link brushless motor mathematical model, the transfer function of the brushless motor can be expressed as:

$$G_2(s) = \begin{bmatrix} \frac{0.75}{0.1s+1} & 0 & 0 & 0 \\ 0 & \frac{0.75}{0.1s+1} & 0 & 0 \\ 0 & 0 & \frac{0.75}{0.1s+1} & 0 \\ 0 & 0 & 0 & \frac{0.75}{0.1s+1} \end{bmatrix}$$

(13)

The transfer function of the system is obtained by multiplying equation (11) with equation (12):

$$G(s) = G_1(s)G_2(s) =$$

$$\begin{bmatrix} \frac{0.75}{sm0.1s+1} & 0 & 0 & 0 \\ 0 & \frac{0.75}{sm0.1s+1} & 0 & 0 \\ 0 & 0 & \frac{0.75}{sm0.1s+1} & 0 \\ 0 & 0 & 0 & \frac{0.75}{sm0.1s+1} \end{bmatrix} \quad (14)$$

According to the actual measured parameters of the hexacopter in Figure 2, the transfer functions of the altitude channel G_Z, roll channel G_H, pitch channel G_F, and yaw channel G_P of the hexacopter aircraft can be obtained as (15) by substituting them into equation (14)

$$\begin{cases} G_Z(s) = \frac{0.4025}{6s(0.1s+1)} \\ G_H(s) = \frac{0.4025}{0.6217s(0.1s+1)} \\ G_F(s) = \frac{0.4025}{0.6217s(0.1s+1)} \\ G_P(s) = \frac{0.4025}{1.0845s(0.1s+1)} \end{cases} \quad (15)$$

The input values for defining the attitude angle are ψ_a, θ_a, and φ_a, and the output feedback angles are ψ, θ, and φ. Therefore, the expression for the error values of e_ψ, e_θ, and e_φ is obtained as (16):

$$\begin{cases} e_\psi = \psi_a - \psi \\ e_\theta = \theta_a - \theta \\ e_\varphi = \varphi_a - \varphi \end{cases} \quad (16)$$

By substituting equation (11) into the PID control expression (10), the control law for attitude angle can be obtained as follows:

$$\begin{cases} \ddot{\psi} = K_p e_\psi + K_i \int_0^t e_\psi \, dt + K_d \frac{d}{dt} e_\psi \\ \ddot{\theta} = K_p e_\theta + K_i \int_0^t e_\theta \, dt + K_d \frac{d}{dt} e_\theta \quad (17) \\ \ddot{\varphi} = K_p e_\varphi + K_i \int_0^t e_\varphi \, dt + K_d \frac{d}{dt} e_\varphi \end{cases}$$

3.4 Fuzzy PID Control Principle

When there are nonlinear models and unknown uncertainties in the control of the system, it is necessary to provide more flexible and intelligent control strategies for

the system. In fuzzy PID controllers, fuzzy logic is used to dynamically adjust PID parameters, enabling the controller to adaptively adjust based on the real-time state of the system, thereby improving control. The structure of the fuzzy PID control system is shown in Figure 5.
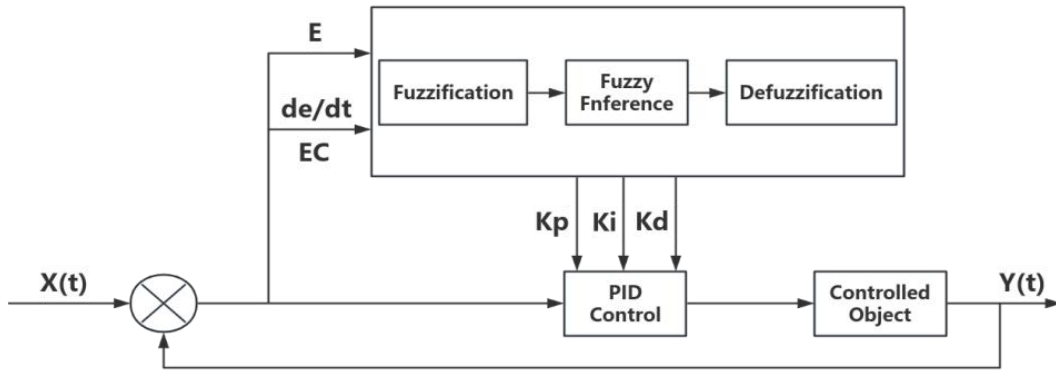
Fig.5 Fuzzy PID Control System Structure Framework Diagram

As shown in Figure 5, fuzzy PID control mainly consists of three steps: fuzzification, fuzzy inference, and deblurring. In a fuzzy PID control system, error E and error rate of change EC are the two inputs of the fuzzy PID controller, while Kp, Ki, and Kd are the three outputs of the controller.

Assuming that the original values Kp1, Ki1, and Kd1 obtained in the classical PID controller are quantized in E and EC, and the correction parameters are determined based on the established fuzzy rules, the resulting correction values are ΔKp, ΔKi, and ΔKd. Finally, they are

multiplied by the scaling factor to output Kp, Ki, and Kd. Therefore, the representation of PID parameters is:

$$\begin{cases} K_p = K_{p1} + \Delta K_p \\ K_i = K_{i1} + \Delta K_i \quad (18) \\ K_d = K_{d1} + \Delta K_d \end{cases}$$

Set the input domain of the fuzzy sets E and EC to [-3 3], and their fuzzy subsets are E=ES={negative large, negative medium, negative small, zero, positive small, median, positive large}={NB, NM, NS, ZO, PS, PM, PB}, with a scaling factor of 1. All inputs and outputs use triangular wave-type membership functions. Establish fuzzy rules based on the fuzzy rule table (Table 2).

Table 2 Fuzzy Rules Table for ΔKp, ΔKi, and ΔKd

$K_P \Delta K_i \Delta K_d$		ES						
		NB	NM	NS	Z0	PS	PM	PB
	NB	PB NB PS	PB NB NS	PM NM NB	PM NM NB	PS NB NB	Z0 Z0 NM	Z0 Z0 PS
	NM	PB NB PS	PB NB NS	PM NM NB	PS NS NM	PS NS NM	Z0 Z0 NS	NS Z0 Z0
	NS	PM NB Z0	PM NM NS	PM NS NM	Z0 NS NM	Z0 Z0 NS	NS PS NS	NS PS Z0
E	Z0	PM NM Z0	PM NM NS	PS NS NS	Z0 Z0 NS	NS PS NS	NM PM NS	NM PM Z0
	PS	PS NM Z0	PS PS Z0	Z0 Z0 Z0	PS NS Z0	NS NS Z0	NM PM Z0	NM PB Z0
	PM	PS Z0 PB	Z0 Z0 NS	PS PS PS	PS NM PS	NM PM PS	NB PB PS	NB PB PB
	PB	Z0 Z0 PB	Z0 Z0 PM	NM PS PM	PM NM PM	NM PM PS	NB PB PS	NB PB PB

3.5 Comparison between Classical PID Control and Fuzzy PID Control

Through Simulink simulation, the control effects of classical PID control systems and fuzzy PID systems can be more intuitively observed, leading to more convincing results. Based on the mathematical model of the dynamics of the hexacopter aircraft calculated in the previous text, substitute the simplified and calculated transfer function equation (15) into the Simulink module. Due to the similarity of the roll channel and pitch channel models, these two channels share a simulation model, and three classical PID control models and three fuzzy PID control models are established. The four channel simulations of classical PID control are shown in Figures 6, 7, and 8. In addition, the simulation models of fuzzy PID control built in Matlab are shown in Figures 9, 10, and 11.

Fig.6 Altitude Channel Simulation Diagram of Classic PID Control for Hexacopter Aircraft
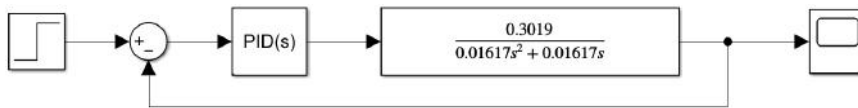
Fig.7 Simulation Diagrams of Roll Channel and Pitch Channel of Classic PID Control for Hexacopter Aircraft

Fig.8 Simulation Diagram of Yaw Channel for Classic PID Control of Hexacopter Aircraft
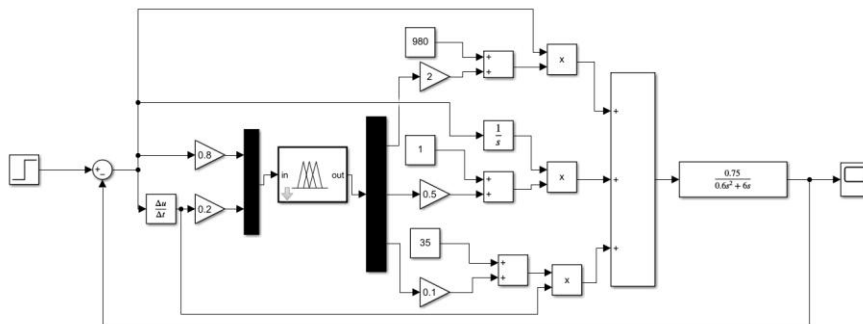
Fig.9 Altitude Channel Simulation of Fuzzy PID Control for Hexacopter Aircraft
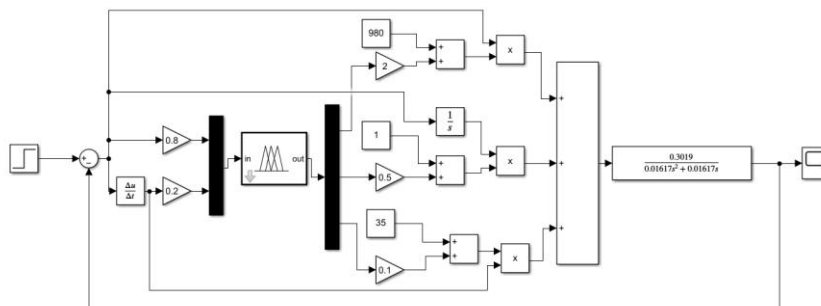
Fig.10 Simulation Diagrams of Roll Channel and Pitch Channel of Fuzzy PID Control for Hexacopter Aircraft
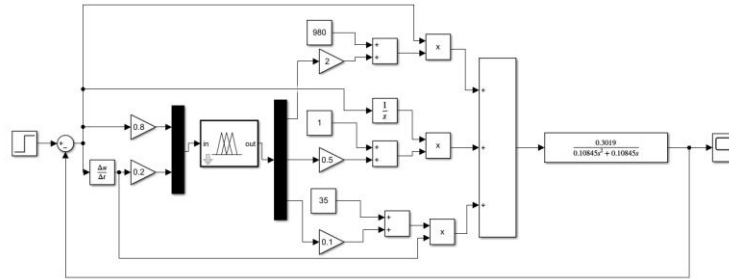
Fig.11 Simulation Diagram of Yaw Channel for Fuzzy PID control of Hexacopter Aircraft

3.6 Hexacopter Simulation Results and Comparison

The K_p, K_i, and K_d values of the classic PID control for the height channel are 180, 12, and 15, respectively; the values of ΔKp, ΔKi, and ΔKd for fuzzy PID control are 1500, 8, and 34, respectively. At a unit-step response, the height channel introduces pulse interference at 0.5 seconds (Figure 12). According to the analysis of the curve changes, it can be seen that fuzzy PID control has a faster response, and under pulse interference, the descent speed is faster. The time to recover stable values is similar, and the time to reach stability is slightly faster than classical PID control.
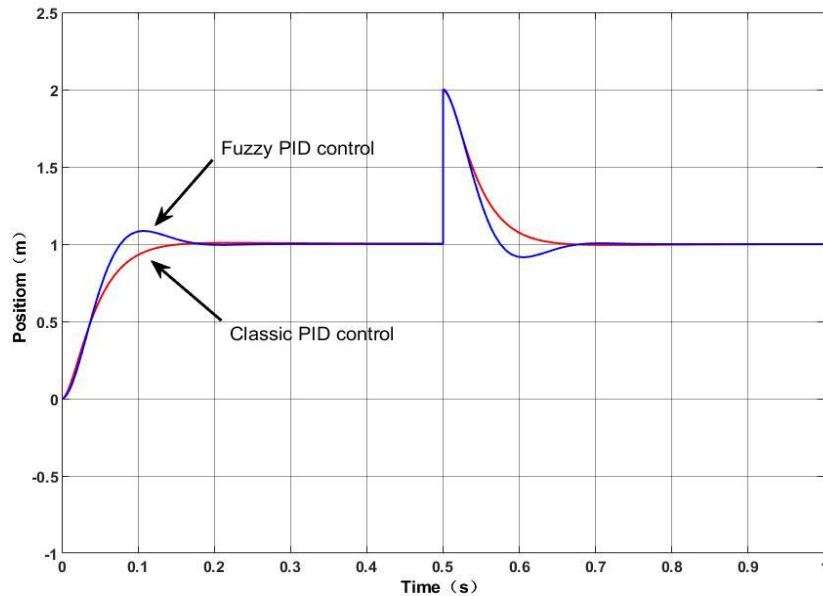
Fig.12 Effect Diagram of Height Channel Pulse Interference Control

The roll channel and pitch channel introduce pulse interference at 0.5 seconds under unit step response (Figure 13). According to the analysis of the curve changes, it can be seen that fuzzy PID control has a faster response, a faster descent speed in the presence of pulse interference, a shorter time required to recover stable values, and a faster time to reach stability than classical PID control.
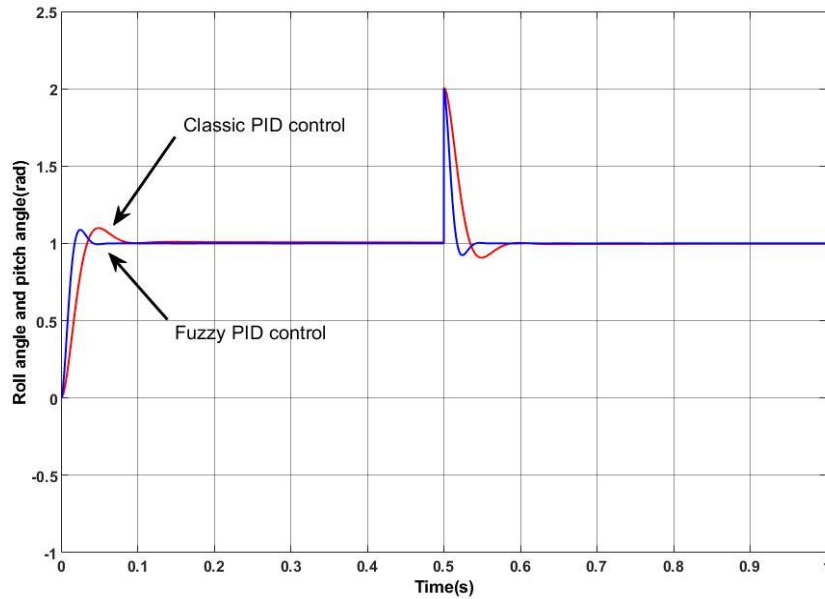
Fig.13 Effect Diagram of Pulse Interference Control for Roll and Pitch Channels

The values of ΔK_p, ΔK_i, ΔK_d for the fuzzy PID control of the yaw channel are 2400, 1, and 38.5, respectively. The yaw channel introduces pulse interference at 0.5 seconds under unit step response (Figure 14). According to the analysis of the curve changes, it can be seen that fuzzy PID control has a faster response. Under pulse interference, its descent speed is faster, and it takes less time to recover stable values. It can be clearly seen that the time to stabilize is faster than classical PID control.
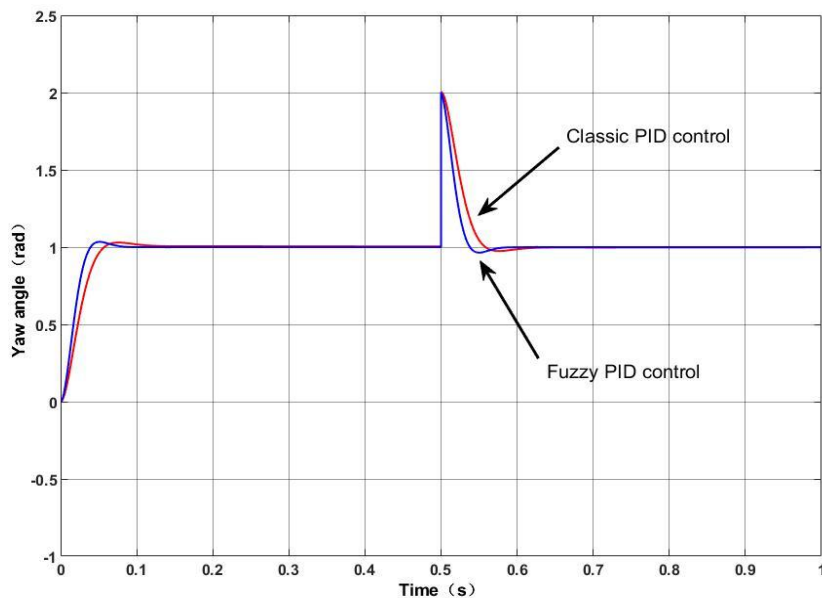
Fig.14 Yaw Channel Pulse Interference Control Effect Diagram

Due to the various uncontrollable factors in the air environment that affect the flight of a hexacopter drone, two continuous signals were selected as interference simulation experiments. Cosine and random numbers were used as input interference signals in Matlab/Simulink simulation, and interference signals were given to the controller at the beginning of the simulation to verify the stability of the control.

According to the simulation curves of the cosine and random interference signals controlled by the height

channel (Figure 15, Figure 16), when the controller is disturbed by the cosine signal, the overshoot of fuzzy PID control is slightly lower than that of classical control, and the adjustment time is shorter. Fuzzy PID can almost be in a relatively stable state, and the response speed of the two is not significantly different. When the controller is disturbed by random signals, although the adjustment time

of classical PID control is shorter than that of fuzzy PID control in some areas, the adjustment time of fuzzy PID is shorter than that of classical PID in most areas. From this, it can be seen that the height channel is relatively stable under fuzzy PID control and can maintain stability by adjusting the interference encountered by the drone in a timely manner.
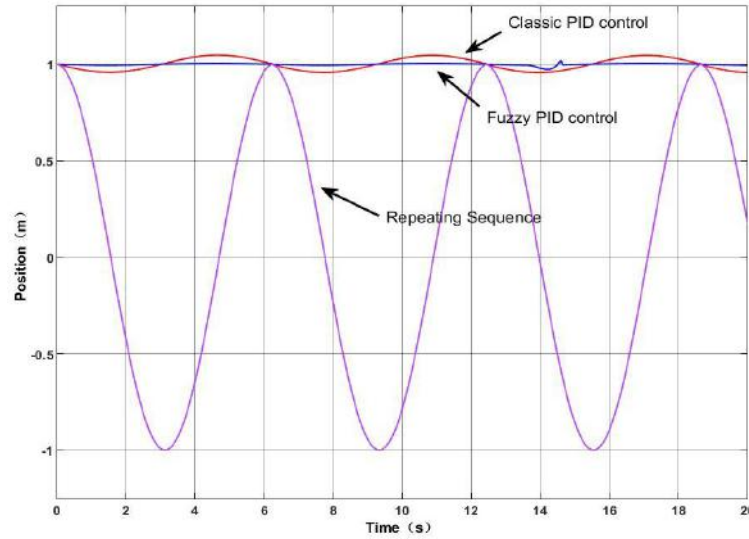
Fig.15 Control Effect Diagram of Cosine Interference Signal in Height Channel
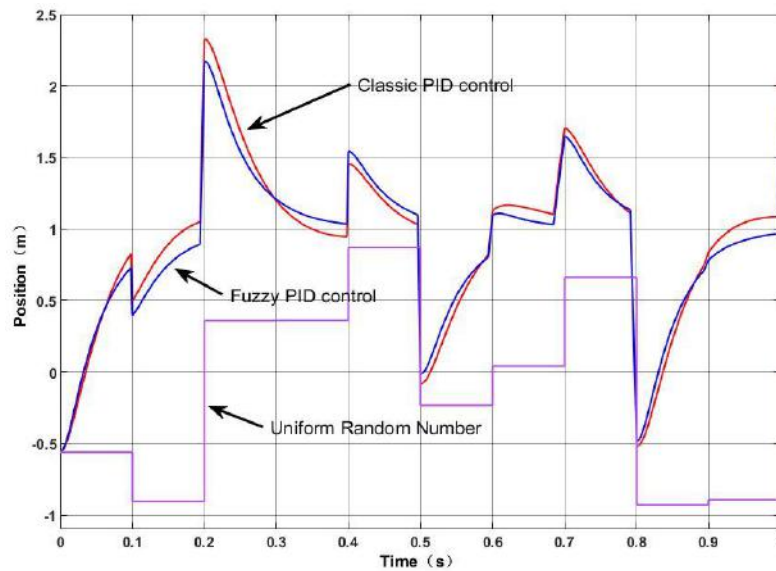
Fig.16 Control Effect of Random Interference Signal in Height Channel

According to the simulated curve changes of cosine and random interference signals for roll and pitch channel control (Figures 17, Figures 18), when the controller is disturbed by cosine signals, the overshoot of fuzzy PID control is slightly smaller than that of classical control, and

the adjustment time is slightly shorter. Fuzzy PID can almost be in a relatively stable state, but there may be slightly larger overshoot, and the response speed of the two is not significant. When the controller is disturbed by random signals, fuzzy PID control has slightly lower

overshoot, faster response speed, and significantly shorter adjustment time than classical control, with shorter rise and fall times, quickly maintaining a stable state. From this, it can be seen that the roll and pitch channels are relatively

stable in fuzzy PID control with a small amplitude difference due to the interference of cosine signals, while the interference comparison effect of random signals is very obvious.
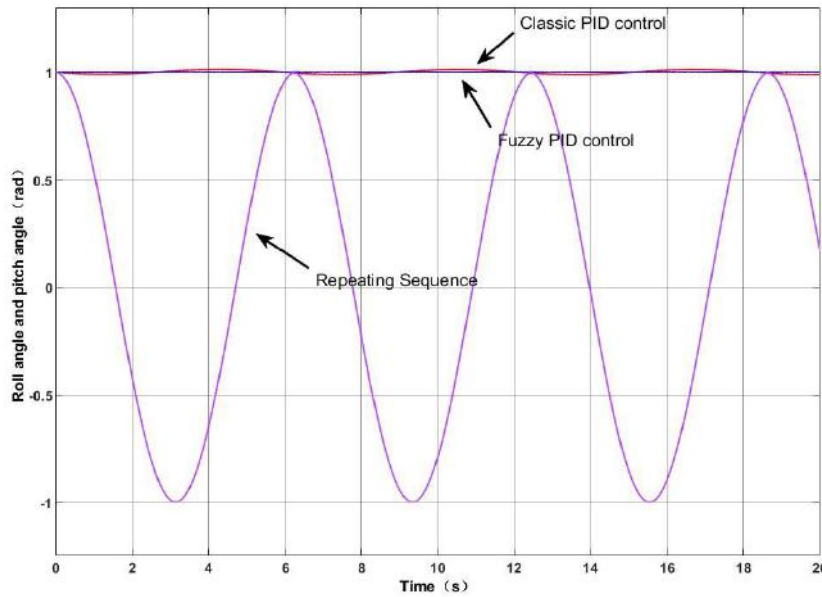
Fig.17 Control Effect Diagram of Cosine Interference Signal in Roll and Yaw Channels
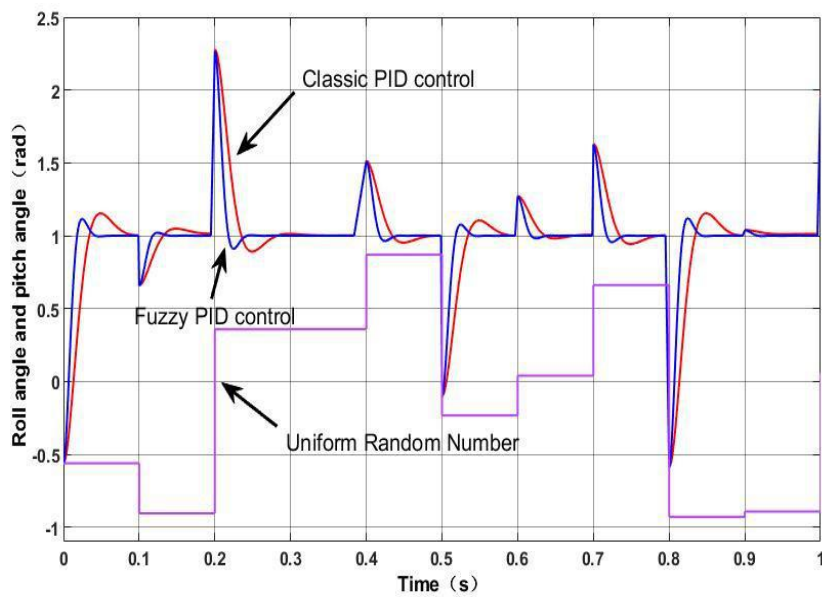
Fig.18 Control Effect Diagrams of Random Interference Signals in Roll and Yaw Channels

According to the simulated curve changes of cosine and random interference signals for yaw channel control input (Figures 19 and Figures 20), when the controller is disturbed by cosine signals, the overshoot of fuzzy PID control is slightly smaller than that of classical control, and the adjustment time is slightly shorter. Fuzzy PID is almost

in a relatively stable state, and the response time of the two is not significantly different. When the controller is disturbed by random signals, the overshoot of fuzzy PID control is almost the same as that of classical control, with relatively fast response speed and shorter adjustment time. The rise and fall times are also significantly shorter, which

can quickly maintain a stable state. From this, it can be seen that the yaw channel is relatively stable under fuzzy
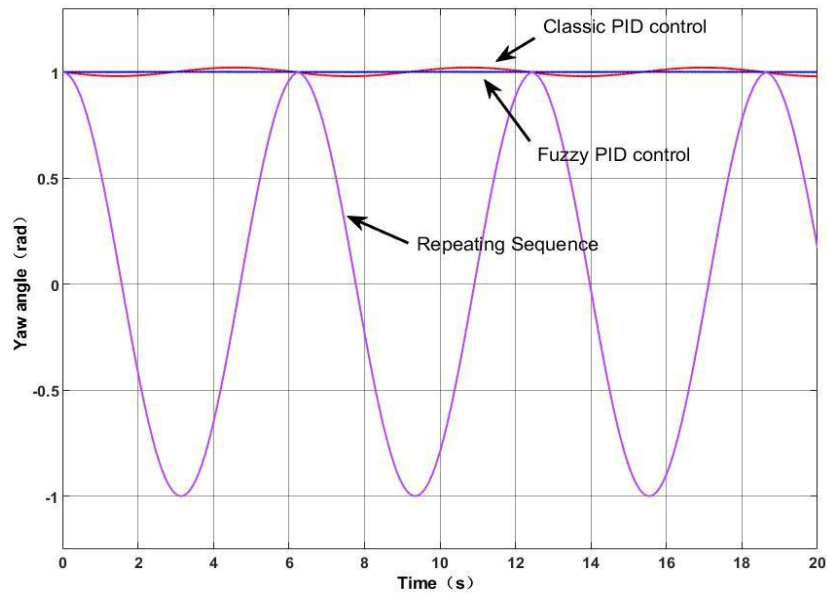
PID control.

Fig.19 Control Effect Diagram of Cosine Interference Signal in Yaw Channel
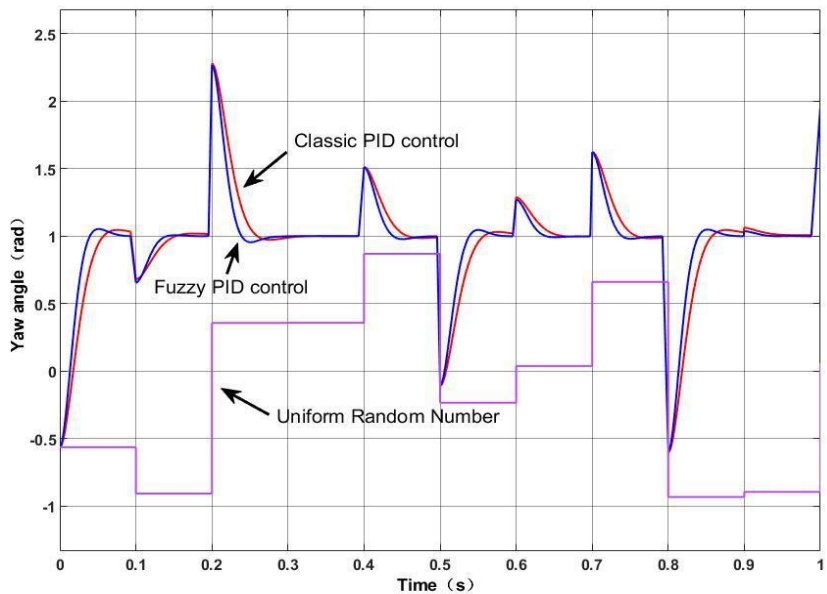
Fig.20 Control Effect of Random Interference Signal in Yaw Channel

IV. CONCLUSIONS

In terms of simulation of hexacopter aircraft under changing real-world conditions, during the actual flight process, drones are subject to many unknown interferences, such as sudden changes in signals, wind resistance, and magnetic fields, which can affect their flight conditions. Therefore, through simulation, problems can be effectively discovered, the design effectiveness of drones can be improved, and the performance of drones can be enhanced.

From the simulation results, it can be seen that if the control system adopts fuzzy PID control, the performance, stability, and anti-interference ability of the hexacopter aircraft are superior to classical PID control. A hexacopter aircraft needs to control the rotation of six motors, and each motor and controller can quickly self-regulate when deviations occur, reducing interference to the drone and

effectively maintaining its ability to fly normally in the air. Overall, the system control is the key to the design of a hexacopter UAVs system. Through the simulation experiment results of this study, ideal scientific data can be obtained to design suitable controllers.

REFERENCES

[1] Alaimo, A., Artale, V., Milazzo, C.L.R. et al., PID Controller Applied to Hexacopter Flight. J Intell Robot Syst. 2014, 73, 261–270. https://doi.org/10.1007/s10846-013-9947-y

[2] Chen, W., Tu, C., Liu, J., Yan, Z., Ren, Y. & Ju, T. Research on Fuzzy PID Flight Control Strategy for Oil Electric Hybrid Hexacopter Unmanned Aerial Vehicle, Journal of Chongqing Jiaotong University (Natural Science Edition). 2024, 43(08):124-132.

[3] Tu, P. Research on fault-tolerant control method for tiltable six rotor unmanned aerial vehicle, East China Jiaotong University. 2023. DOI:10.27147/d.cnki.ghdju.2023.000373.

[4] Lopez-Franco, C., Gomez-Avila, J., Alanis, A.Y., Arana-Daniel, N., and Villaseñor, C., Visual Servoing for an Autonomous Hexarotor Using a Neural Network Based PID Controller. Sensors. 2017, 17(8):1865. https://doi.org/10.3390/s17081865

[5] Tang, M., Fesign of Water Quality Sampling Unmanned Aerial Vehicle System Based on Fuzzy PID, Nanjing University of Information Science and Technology. 2021. DOI:10.27248/d.cnki.gnjqc.2021.000861.

[6] Yao, S., Research on Hardware Control System Design and Attitude Control Optimization of Six rotor Agricultural Patrol Carrier Drone, Xinjiang Agricultural University. 2023. DOI:10.27431/d.cnki.gxnyu.2023.000213.

[7] Zhao, J., Chen, Z., and Zhang, R. Research on Multi rotor Precise Fixed point Hover Control Based on Cascade PID. 2021, 28(08):17-20+30.

[8] Perez-Saura, D., Fernandez-Cortizas, M., Perez-Segui, R. et al. Urban Firefighting Drones: Precise Throwing from UAV. J Intell Robot Syst. 2023, 108, 66. https://doi.org/10.1007/s10846-023-01883-6

[9] Shen, W. Research on pose detection of hexacopter unmanned aerial vehicle based on visual assistance. 2021. DOI: 10.27234/d.cnki.gnhuu.2021.000401.

[10] Yang, B. Research on the Application and Development of Multi rotor Drones in the Rescue Field. Computer Products and Distribution. 2020, (05):130.

[11] Wang, C., Application and Development Trend Analysis of Multi rotor Drones in Military Logistics Field, Winged missile. 2021, (08):56-60. DOI:10.16338/j.issn.1009-1319.20200334.

[12] He, Z. Research on UAV flight control and communication method based on fuzzy adaptive. Wireless Netw. 2024, 30, 6105–6113. https://doi.org/10.1007/s11276-023-03408-3

[13] Li, S., He, D., and Liao, F. Attitude stabilization backstepping control of a six rotor unmanned aerial vehicle based on nonlinear feedforward compensation. 2024, 1-21. https://doi.org/10.16183/j.cnki.jsjtu.2023.652.

[14] Ding, L., Wu, H., and Li, X. Trajectory Tracking Control of Hexacopter Aircraft under Aggregate Interference. 2018, 40(05): 622-628. DOI:10.13374/j.issn2095-9389.2018.05.013.

[15] Chen, Y. Research on fault-tolerant flight control of hexacopter unmanned aerial vehicles, Nanjing University of Aeronautics and Astronautics, 2014.